

Decoupled Conflict-Resolution Procedures for Decentralized Air Traffic Control

Santosh Devasia, Dhanakorn Iamratanakul, Gano Chatterji, and George Meyer, *Life Fellow, IEEE*

Abstract—This paper addresses the challenge of designing provably safe conflict-resolution procedures (CRPs) that are decentralized and decoupled from each other. The main contribution of this paper is identifying necessary and sufficient conditions to decouple CRPs. Additionally, this paper demonstrates the existence of decentralized en-route CRPs that satisfy the identified decoupling conditions for each local conflict and, thereby, guarantee global conflict resolution. An advantage of the proposed CRPs is that they do not require a reduction in the aircraft flow levels in the intersecting routes for conflict resolution, which can aid in increasing the efficiency of en-route air traffic control.

Index Terms—Air traffic control, conflict decoupling, conflict resolution, distributed algorithms, distributed control, domino effect.

I. INTRODUCTION

THIS PAPER addresses the decoupling of conflict-resolution procedures (CRPs) for decentralized en-route air traffic control (ATC). CRPs tend to be decentralized (spatially and temporally) because of the substantial increase in computational and modeling complexity with a centralized CRP when the number of aircraft (and conflicts) increases. Additionally, centralized controllers become inefficient, over large airspace, because of the need to handle the uncertainty in aircraft trajectories over time, e.g., due to the sensitivity of predicted ground speeds to wind and temperature forecasts [1], which in turn depend on the forecasts of dynamic weather conditions with substantial uncertainties [2]. Therefore, decentralized CRPs are needed to resolve conflicts to manage the complexity and uncertainty in ATC. A major challenge, however, is to ensure that modifications of flight trajectories, to resolve a conflict, do not lead to a *domino* effect, i.e., the resolution of a conflict should not lead to new conflicts, whose resolution leads to additional conflicts, and so on [3]. The main contribution of this paper is identifying necessary and

sufficient conditions to decouple CRPs. Additionally, this paper demonstrates the existence of decentralized en-route CRPs that satisfy the decoupling conditions for each local conflict and, thereby, guarantee global conflict resolution. An advantage of the proposed CRPs is that they do not require a reduction in the aircraft flow levels in the intersecting routes for conflict resolution, which can aid in increasing the efficiency of en-route ATC.

Improvements in en-route CRPs can help increase the efficiency of ATC in congested parts of the airspace. Congestions arise, e.g., due to merges in current approaches used for managing adverse weather conditions [4], [5]. Under current traffic flow management, standardized procedures in the National Severe Weather Playbook [6]–[8] allow aircraft to be rerouted around a region with adverse weather. For route simplicity, air routes (even those going to different destinations) tend to be merged before rerouting around the adverse weather region. For example, Fig. 1(a) shows the “West Watertown” procedure [6] used to merge and reroute aircraft from the west coast when a large area in the Midwest is affected by adverse weather. Merges simplify conflict resolution in nearby regions (e.g., with the preexisting route represented by a dashed line in Fig. 1) and ease the interfacing with human controllers. However, restrictions on the acceptable aircraft flow level on the merged route lead to a reduction of the acceptable aircraft flow levels in the routes that are merged [6]. In contrast, it might be possible to design reroutes that avoid the reduction in aircraft flow levels (by avoiding merges) in the routes that aim to pass through the affected region, e.g., as illustrated in Fig. 1(b). The increase in number of reroutes (when compared with the case with merges) can increase the number of intersections with preexisting routes in the nearby region. The complexity of ATC in such congested regions could be reduced with the proposed CRPs, at each intersection, since the CRPs are decoupled from each other. Furthermore, the proposed CRPs do not require a reduction in the aircraft flow levels (i.e., capacity of the reroutes) for conflict resolution, which improves the ATC efficiency when compared with existing merge-based procedures.

Automation to assist human controllers can lead, in general, to reduced workload and improved efficiency, as shown in [9]–[13]. For example, automation tools to schedule and resolve conflicts for aircraft arriving at an airport terminal have been developed by researchers at the National Aeronautics and Space Administration Ames Research Center [9]. Researchers are also developing automation tools to detect and resolve en-route conflicts (see, e.g., [9] and [14]–[19]) under the free flight paradigm [9], [10], which can eventually enable different airline operational centers to negotiate with each other for minimizing

Manuscript received May 4, 2009; revised July 26, 2010; accepted November 3, 2010. Date of publication February 10, 2011; date of current version June 6, 2011. This work was supported by the NASA Ames Research Center under Grant NAG 2-1277, Grant NAG 2-1450, and Grant NNA04C131G. The Associate Editor for this paper was J.-P. B. Clarke.

S. Devasia and D. Iamratanakul are with the University of Washington, Seattle, WA 98195-2600 USA (e-mail: devasia@u.washington.edu; na@u.washington.edu).

G. Chatterji and G. Meyer, retired, are with the Ames Research Center, National Aeronautics and Space Administration, Moffett Field, CA 94087 USA (e-mail: Gano.B.Chatterji@nasa.gov; george.meyer@sbcglobal.net).

Color versions of one or more of the figures in this paper are available online at <http://ieeexplore.ieee.org>.

Digital Object Identifier 10.1109/TITS.2010.2093574

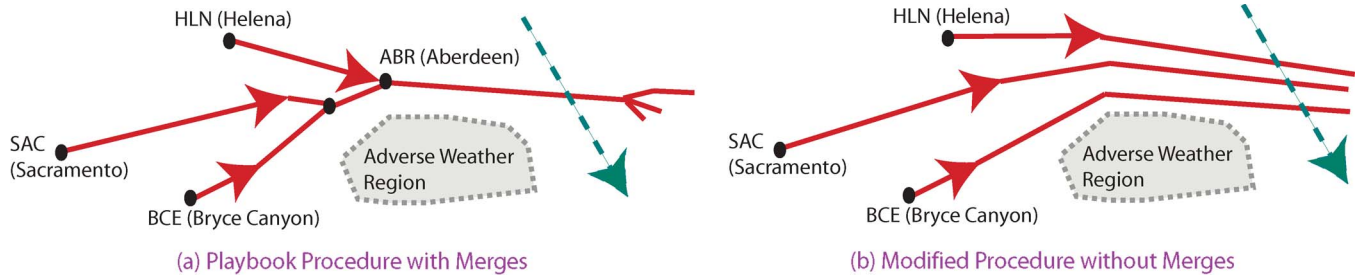


Fig. 1. Rerouting procedures with and without merges. Plot (a) “West Watertown” procedure (figure adapted from [6]) used to merge and reroute aircraft around an adverse weather region. Dashed line represents a preexisting route in the nearby region. Plot (b) reroutes without merges increase ATC complexity and can benefit from improved en-route CRPs. (a) Playbook procedure with merges. (b) Modified procedure without merges.

operational costs, e.g., [20]. The challenge, in the development of automation tools for CRPs, is to show that the automated procedure will always lead to a solution of the conflict-resolution problem for guaranteeing safety. This paper develops a framework for the design of such provably safe CRPs.

Previous works on automated CRPs range from nonlocal probabilistic approaches that handle uncertainties [21] to local deterministic approaches that resolve conflicts in a collaborative manner [22], [23]. Analytical issues such as proving the local safety of conflict resolution were studied in, e.g., [24]. The problem of guaranteed conflict resolution in a stable manner remains more challenging for the nonlocal case. For example, procedures to resolve conflicts between aircraft along intersecting routes might not be stable, as shown in [25]. Previous works have developed stable CRPs for two and three intersecting routes [23], [25]. The main difficulty is that decentralized procedures for individual intersecting routes interact with adjacent intersections. Solving the resulting coupled problem, in a stable manner, can require centralized solutions [25]. In contrast, the current work seeks decentralized procedures that guarantee conflict resolution with multiple conflicts (intersections) by using decoupled procedures—the cost of this guarantee is time delay with known bounds.

This paper focuses on conflict resolution along prespecified aircraft routes, as in [14], [26], and [27]. Such *highway-like* routes, if sufficiently dense in the airspace and variable over time [28], could provide sufficient flexibility for accommodating weather patterns [29], missed connections, and traffic congestion by choosing desired flight segments along the route structure in a free-flight-like setting. Global resolution of all the intersecting conflicts in any given route structure can be achieved if the local CRP designs, at each of the route intersections, are decoupled from each other. Towards such decentralized global conflict resolution in intersecting routes, this paper extends previous efforts [30], [31] by identifying necessary and sufficient conditions for decoupled CRPs.

This paper demonstrates the existence of decentralized en-route CRPs (based on [30] and [31]), which satisfy the decoupling conditions. Such decoupled CRPs can be useful as a nominal solution for getting the distribution of bounds on delays in the airspace for a given global route structure and, thereby, enable optimization of the route structures. Note that the computational effort for the global conflict resolution linearly grows with the number of conflicts since the local CRPs are decoupled from each other.

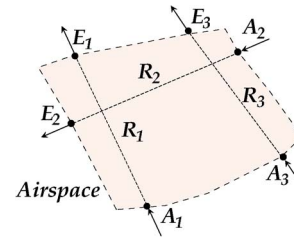


Fig. 2. Route description. Three routes $\{R_1, R_2, R_3\}$ are shown, along with the associated arrival points $\{A_1, A_2, A_3\}$ and exit points $\{E_1, E_2, E_3\}$.

II. CONDITIONS FOR DECOUPLED CONFLICT RESOLUTION PROCEDURES

In this section, we formulate the conflict-resolution problem and develop necessary and sufficient conditions for CRPs to be decoupled.

A. Airspace Description

The airspace \mathcal{AS} , where conflicts are to be resolved, is assumed to be at a fixed altitude (planar flight) in which aircraft fly, with a constant speed v_{sp} , along one of a predefined set of distinct routes $\mathcal{R} = \{R_i\}_{i=1}^n$ with arrival points $\mathcal{A} = \{A_i\}_{i=1}^n$ and exit points $\mathcal{E} = \{E_i\}_{i=1}^n$. As illustrated in Fig. 2, each route $R_i \in \mathcal{R}$ is a directed path (not necessarily a straight line) from an arrival point $A_i \in \mathcal{A}$ to an exit point $E_i \in \mathcal{E}$. Moreover, the maximal length r_{\max} of all routes $R_i \in \mathcal{R}$ in the airspace is assumed to be finite, which implies that the nominal time to traverse the airspace along any route (without accounting for intersections) is finite and less than

$$T_{\max} = r_{\max}/v_{sp}. \quad (1)$$

Assumption 1 (Initially Conflict Free): Aircraft arriving at a route R_i (at each arrival point A_i) are separated by at least distance \underline{d} that is greater than the minimum required separation d_{sep} , i.e., $\underline{d} > d_{\text{sep}} > 0$.

Remark 1: Sorting of aircraft flows into a layered structure at different altitudes, with similar flight direction (such as east to west) and fixed nominal speed in each altitude, simplifies the management of air traffic. Although such layering is present in current air traffic management, conflict resolution is still needed when aircraft flows cross each other inside a layer—these crossings cannot be avoided due to the limited number of altitude layers available to separate flows.

B. Definition of Local Conflict Regions

The goal is to develop decoupled CRPs to avoid conflicts between aircraft on different routes, where the conflict points in the airspace are separated into local conflict regions (which are defined formally as follows).

Definition 1 (Conflict Point): A conflict point is any point on a route that is less than the minimal separation distance d_{sep} from a point on another route.

All conflict points, in the airspace under consideration, are grouped inside a finite number N_L of local conflict regions $\mathcal{L} = \{L_i\}_{i=1}^{N_L}$. For simplicity, it is assumed that the local conflict regions are circular discs that are strictly contained in the airspace (i.e., $\mathcal{L} \subset \mathcal{AS}$), do not include the arrival points \mathcal{A} and exit points \mathcal{E} of the routes \mathcal{R} in the airspace, and satisfy the following conditions.

Assumption 2 (Conditions on Local Conflict Regions):

- 1) Simple: Each local conflict region L_i contains exactly two distinct routes $R_{i,1} \in \mathcal{R}$ and $R_{i,2} \in \mathcal{R}$.
- 2) Bounded: Each conflict region L_i is assumed to be a bounded disc of radius $r_i \geq d_{\text{sep}}$ centered around a point p_i .
- 3) Disjoint: The intersection of any two local conflict regions is empty, i.e., $L_i \cap L_j = \emptyset$ if $i \neq j$.

Remark 2: The bounded condition (in Assumption 2) and the requirement that the exit point not be in the conflict region imply that the problem does not consider merging routes. Merges could be handled, for example, using automation tools developed to schedule aircraft arriving at an airport terminal, e.g., [9] and [32]. It is noted that, in general, en-route merges tend to reduce the flow capacity of the merged routes. Some merges (e.g., use to maintain ATC simplicity) could be avoided in future paradigms if automated en-route CRPs can be developed to handle the increased ATC complexity.

Remark 3: The disjoint condition aims to allow sufficient space for local CRPs to be decoupled from each other.

C. Formulation of Decoupled Conflict-Resolution Problem

The problem is to locally resolve conflicts that arise between aircraft on different routes provided the routes (and, therefore, the conflict regions) are sufficiently sparse.

Definition 2 (κ -Sparse Airspace): The airspace is κ sparse (where $\kappa \geq 1$) if, for each local conflict region L_i (center p_i , radius r_i , and routes $R_{i,1} \in \mathcal{R}, R_{i,2} \in \mathcal{R}$), the concentric disc B_i of radius κr_i and center p_i (see Fig. 3) is as follows.

- 1) It is strictly contained in the airspace $B_i \subset \mathcal{AS}$.
- 2) It only contains the two routes $R_{i,1}$ and $R_{i,2}$ with corresponding unique arrival points $A_{i,1}, A_{i,2} \in B_i$ and unique exit points $E_{i,1}, E_{i,2} \in B_i$ on the routes, as shown in Fig. 3.
- 3) It is separated by at least the minimum required distance d_{sep} from all other routes, e.g., $d_1 \geq d_{\text{sep}}$ in Fig. 3.
- 4) It is disjoint and conflict free from other discs, i.e., separated from any other disc B_j (of radius κr_j and center p_j) by at least the minimal separation distance d_{sep} .

Remark 4: If the airspace is κ -sparse, then local CRPs can change the route structure inside the disc B_i (which is larger

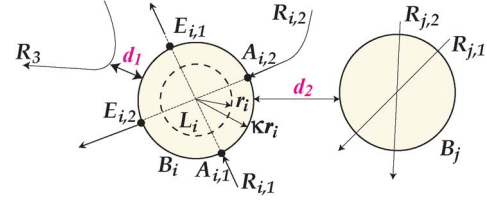


Fig. 3. Local conflict region L_i and associated disc B_i with routes $R_{i,1}, R_{i,2}$. The distance of the disc B_i from other routes (other than $R_{i,1}, R_{i,2}$, e.g., distance d_1 from R_3 in the figure) and other local discs (e.g., d_2 from B_j) is at least the minimal separation distance d_{sep} .

than the local conflict region L_i) without causing additional local conflicts with other routes.

A local CRP ensures safety locally, i.e., aircraft spacing is maintained to be at least the minimal separation distance d_{sep} inside a local region—this is defined formally as follows.

Definition 3 (\underline{d} -Type Local Conflict Resolution): Given a κ -sparse airspace, a local conflict region L_i , and its associated disc B_i , a \underline{d} -type local CRP C_{L_i} (that modifies aircraft path only within the disc B_i) ensures that the aircraft will leave the disc B_i with constant nominal speed v_{sp} and without conflicts inside the disc B_i provided the aircraft arrive at the nominal arrival points ($A_{i,1}, A_{i,2}$ of routes $R_{i,1}, R_{i,2}$) separated from each other by at least distance \underline{d} .

Remark 5: A local CRP C_{L_i} does not guarantee absence of conflicts outside the local area, i.e., outside disc B_i .

The objective is to design local CRPs that prevent conflicts globally (i.e., in the entire airspace \mathcal{AS} under consideration).

Definition 4 (Decoupled, Global Conflict Resolution): Given a κ -sparse airspace \mathcal{AS} , a set of \underline{d} -type local CRPs $\mathcal{C}_{\mathcal{L}} = \{C_{L_i}\}_{i=1}^{N_L}$ is considered to be a decoupled global conflict resolution if the following conditions are met.

- 1) Safety: There are no conflicts (i.e., separation between aircraft is at least the minimum d_{sep}) in the entire airspace.
- 2) Decoupling: The procedures used in each local conflict resolution C_{L_i} (such as route changes inside B_i) are independent of the procedures used at other locations (e.g., C_{L_j} in B_j).
- 3) Liveness: Passage through the airspace (to the intended destination, i.e., aircraft on route R_i exit at the corresponding exit point E_i with minimal spacing \underline{d}) is guaranteed within a specified maximum time $T_{\text{max}} < \infty$.
- 4) Fairness: The passage through the airspace is on a first-come-first-served (FCFS) schedule for each route, i.e., the sequence of aircraft arrival on a particular route is maintained at the exit point of the route from the airspace.

Remark 6: The liveness and fairness conditions are not required for safe separation; however, liveness implies that aircraft will not be stuck in the airspace (e.g., in a loop), and fairness enables acceptance of the CRP. The FCFS scheduling of aircraft is considered as the canonical fair schedule in air traffic management [33].

Remark 7: The proposed (FCFS-based) CRPs will not result in unwanted changes in schedule. However, if an intentional reordering of aircraft sequence is desired, then the proposed CRPs can be integrated with existing procedures to swap

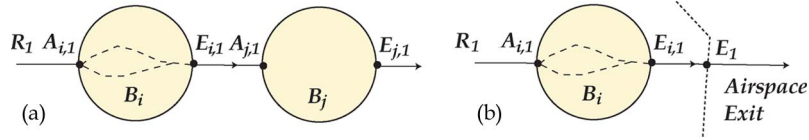


Fig. 4. Local intent requires that aircraft arriving at $A_{i,1}$ in route R_1 merge before exiting at $E_{i,1}$ in conflict disc B_i . (a) Route R_1 enters another conflict disc B_j after current conflict disc B_i . (b) Route R_1 exits the airspace after current conflict disc B_i .

aircraft order, e.g., by delaying one of the aircraft using path extensions. Such reordering procedures are separate from the conflict-resolution problem considered in this paper.

D. Conditions for Existence of Solutions

Necessary and sufficient conditions for the existence of a solution to the decoupled global conflict-resolution problem are presented in the following lemma.

Lemma 1: Given any κ -sparse airspace \mathcal{AS} , a set of \underline{d} -type local CRPs $\mathcal{C}_{\mathcal{L}}$ will satisfy the conditions for decoupled global conflict resolution (see Definition 4) if and only if the following *local* conditions are satisfied. For any local conflict region L_i and its associated disc B_i (as in Fig. 3), aircraft arrive at arrival points $A_{i,1}$ and $A_{i,2}$ separated from each other by at least distance \underline{d} , and we have the following:

- 1) local intent: aircraft on each route in the disc B_i exit along the route at the corresponding exit point $E_{i,1}, E_{i,2}$;
- 2) local liveness: aircraft on each route in the disc B_i exit the disc within a specified maximum time $T_i < \infty$;
- 3) local fairness: the passage through the disc B_i is FCFS within each route;
- 4) local exit spacing: aircraft exiting the disc (at each of the two exit points) are separated by at least distance \underline{d} .

Proof: The proof consists of two parts: 1) sufficiency and 2) necessity.

(i) Sufficiency:

Global Safety: Local intent and local exit spacing are sufficient conditions for global safety. Local conflict resolution C_{L_i} prevents conflicts inside the local conflict disc B_i ; if the aircraft leave along the intended routes with spacing $\underline{d} > d_{\text{sep}}$, then there are no conflicts along the route until the next local conflict disc along the route, for example, B_j . The local exit spacing condition allows compatibility between local CRPs because it ensures that the spacing of aircraft arriving at B_j (at one of the arrival points $A_{j,1}$ or $A_{j,2}$) is at least \underline{d} . This arrival spacing of \underline{d} is compatible with the next CRP C_{L_j} to avoid conflicts in the next local disc B_j . The repetition of this argument for each local conflict region along each route guarantees that there are no conflicts in the entire airspace under consideration.

Global Liveness: The time needed for aircraft on any single route to reach the intended exit point of the airspace can be bounded by $T_{\max} + \sum_{i=1}^{N_L} T_i$ [where T_{\max} is the maximum time needed without conflicts, as in (1)], thus guaranteeing global liveness.

Global Fairness: Local fairness is sufficient for global fairness since the sequence of aircraft in each route is maintained through each local CRP.

Decoupling: The local CRPs are decoupled through the local exit spacing condition that ensures compatibility between two successive local CRPs. The only requirement to ensure that the next local CRP can manage its potential local conflicts is that the aircraft arrive sufficiently spaced (by \underline{d}), i.e., aircraft leave the current local disc sufficiently spaced (by \underline{d}). It is noted that this is a local condition that helps to ensure decoupling between sequential CRPs.

(ii) Necessity:

Local Intent: Necessity of local intent arises from the need to ensure that aircraft on a specific route, for example, R_1 , converge back to that route by only using local CRPs with resolution procedures inside each conflict disc, i.e., without additional procedures outside the conflict discs. If, after the conflict disc B_i , the route R_1 enters another conflict disc B_j , as in Fig. 4(a), then convergence of aircraft back to the nominal route R_1 is needed before B_j to satisfy the arrival condition at the next CRP C_{L_j} (see Definition 3)—the arrival condition ensures that CRPs C_{L_i} and C_{L_j} are decoupled. On the other hand, if, after the conflict disc B_i , the route R_1 exits the airspace, as in Fig. 4(b), then convergence back to the nominal route R_1 is needed to satisfy the global liveness condition. In either case, the CRP C_{L_i} is local, and changes cannot be made to the routes outside of the conflict disc. Therefore, convergence back to the nominal route (local intent) needs to be completed within the conflict disc of each local CRP.

Local Liveness: If local liveness is not satisfied in one local disc B_i , i.e., the time T_i needed to leave the local disc B_i is not finite, then the time needed to leave the airspace is also not finite.

Local Fairness: If the sequence of aircraft departing a local disc B_i is not the same as the arrival sequence, then the sequence has to be changed for global fairness. The sequence cannot be changed outside of the local discs because of the local nature of CRPs, which only allows path deviations inside of the local discs. If the sequence is to be changed inside a different local disc, then the procedures of the two discs become coupled, thereby violating the decoupling requirement.

Local Exit Spacing: If the aircraft exit a conflict disc B_i with separation less than \underline{d} , then it violates the arrival spacing condition at the next conflict disc, for example, B_j in a general airspace, for guaranteed conflict resolution in B_j . If the aircraft leave the airspace after B_i , then the local exit spacing is needed to meet the spacing requirement when leaving the airspace because changes are not allowed outside of B_i . ■

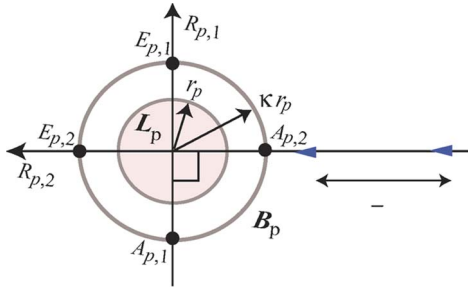


Fig. 5. Two perpendicularly intersecting routes $R_{p,1}$ and $R_{p,2}$. The conflict region L_p has radius $r_p = d_{sep}$, the associated conflict disc B_p has radius κr_p , and aircraft arrive at $A_{p,1}$ and $A_{p,2}$ separated by at least $\underline{d} > d_{sep}$.

Corollary 1 (Complex Conflicts): The conditions for decoupled CRP in Lemma 1 are also applicable for complex conflicts, i.e., when each conflict region L_i potentially contains more than two distinct routes and more than one intersection—as opposed to simple conflicts in Assumption 2.

Proof: The proof is similar to that of Lemma 1. ■

Remark 8: The local nature of the CRPs plays an important role in the foregoing necessity argument. The rationale for requiring the CRP to be local (i.e., procedures should be inside of the local conflict discs) is that if the aircraft paths are to be changed outside of the local discs, then there is no guarantee that the procedure will not lead to additional conflicts along the routes in a general air space; resolving these would violate the ability to design the CRPs in a decentralized decoupled manner over the airspace.

Remark 9: The foregoing results could be generalized to 3-D flows (and 3-D CRPs, e.g., see [34]) by considering 3-D local conflict regions rather than 2-D discs. New issues in such a generalization would include variations in speed and differing separation standards. Nevertheless, the concepts introduced in the foregoing results such as the need for local intent, liveness, fairness, and exit spacing can be applicable to such generalizations. The current study, however, only demonstrates a 2-D decoupling CRP (which satisfies the necessary and sufficient conditions for decoupling as in Lemma 1) for planar flows.

III. DECOUPLED CONFLICT RESOLUTION PROCEDURES

In this section, we establish the existence of decoupled global CRPs (see Definition 4) by demonstrating a local CRP that satisfies the necessary and sufficient conditions for decoupling as in Lemma 1. For ease in exposition, this section considers the problem of perpendicularly intersecting routes.

A. Perpendicularly Intersecting Routes

Consider the conflict-resolution problem for a local conflict region L_p of radius $r_p = d_{sep}$ with two straight-line routes $R_{p,1}$ and $R_{p,2}$ that intersect perpendicularly, as shown in Fig. 5.

In general, conflict resolution can be achieved using maneuvers that change the heading, speed, and altitude. However, heading changes are preferred over speed changes, which cost additional fuel for accelerating and decelerating the aircraft. Similarly, heading changes are preferred over altitude changes, which tend to incur passenger discomfort and can cause con-

flicts in the other altitudes [23], [26]. Therefore, this section develops a heading-change-based CRP.

Assumption 3 (Turn Dynamics): In the following, the turn dynamics is not modeled and heading changes are considered to be instantaneous (as in [23], [26], and [35]) when designing the route modifications for conflict resolution.

The conflict-resolution problem for the perpendicular intersection is stated below.

Definition 5 (Decoupling Perpendicular CRP Problem): Find a local CRP that satisfies the decoupling conditions (see Lemma 1) by only using heading change maneuvers for the perpendicularly intersecting routes, i.e., conflict region L_p (in Fig. 5) when aircraft arrive (at $A_{p,1}$ and $A_{p,2}$) with a separation distance of at least \underline{d} . The radius r_p of the conflict region L_p is considered to be the minimum separation distance d_{sep} .

B. Admissible Heading Change Maneuver

The following lemma (adapted from [2] and [26]) relates the admissible (conflict-free) heading change to the separation between aircraft.

Lemma 2 (Minimum Separation for Heading Change): Consider two aircraft (a_1, a_2) with the same speed along a straight line route, as shown in Fig. 6(a). Let aircraft a_1 change its heading by ϕ and aircraft a_2 continue in a straight line. Then, the minimum spacing d_{min} between the two aircraft to avoid conflict is given by

$$d_{min} = \frac{d_{sep}}{\cos(\phi/2)}. \quad (2)$$

Proof: The relative motion of aircraft a_1 with respect to aircraft a_2 is given by the vector $V_{a_1} - V_{a_2}$, as shown in Fig. 6(b). Therefore, a safety disc (of diameter d_{sep}) centered around aircraft a_1 generates the shaded area in Fig. 6(a) that is bordered by two parallel lines separated by d_{sep} and centered along the vector $V_{a_1} - V_{a_2}$. For conflict avoidance, the safety disc around aircraft a_2 (of diameter d_{sep}) should not intersect the shaded area associated with the relative motion of the safety disc of aircraft a_1 . Therefore, the minimal safe distance d_{min} between aircraft occurs when the safety disc around aircraft a_2 just touches the shaded area, as shown in Fig. 6(b). The angle β made by the relative velocity vector $V_{a_1} - V_{a_2}$ with respect to the horizontal in Fig. 6(b) can be found from the isosceles triangle $\Delta(Fa_1E)$ in Fig. 6(a) as

$$\beta = (\pi + \phi)/2. \quad (3)$$

The current lemma follows from the right-angled triangle $\Delta(a_1Ca_2)$ in Fig. 6(b), which yields

$$\sin(\pi - \beta) = \frac{d_{sep}}{d_{min}} \quad (4)$$

where $\sin(\pi - \beta) = \cos(\phi/2)$ from (3). ■

Corollary 2 (Admissible Heading Change): Consider two aircraft (a_1, a_2) with the same speed along a straight line route and separated by distance $d > d_{sep}$, as shown in Fig. 6(a). A fixed heading change Φ of aircraft a_1 is admissible (i.e., does not lead to conflict when aircraft a_2 continues in a straight line)

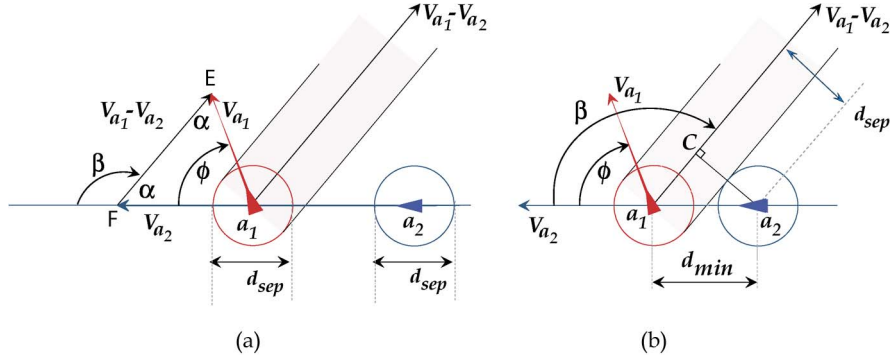


Fig. 6. (a) Relative motion of aircraft a_1 with respect to aircraft a_2 when aircraft a_1 changes heading by ϕ . (b) Minimum separation d_{min} between aircraft to avoid conflict.

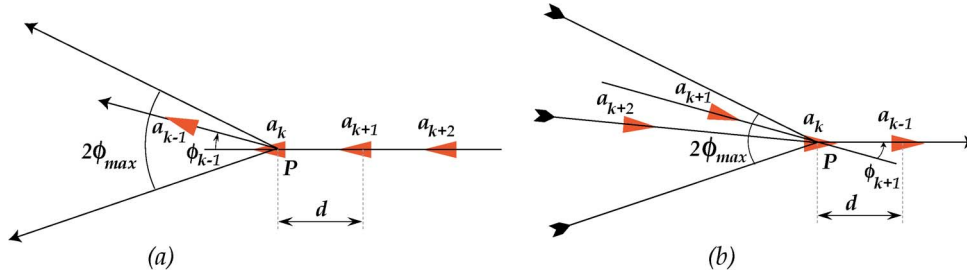


Fig. 7. Diverging/converging aircraft. (a) Aircraft diverge from point P with heading angle Φ . (b) Aircraft converge to point P .

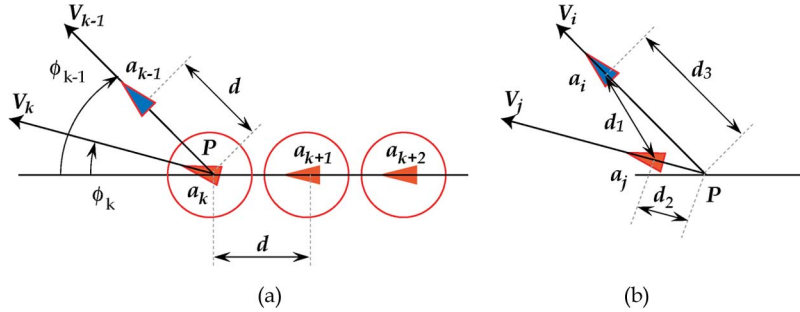


Fig. 8. (a) Diverging sequence (plot shows minimal spacing d), where aircraft a_{k-1} has heading angle ϕ_{k-1} , and aircraft a_k has heading angle ϕ_k . (b) Spacing between two aircraft a_i and a_j that have passed the heading change point P .

if the heading change Φ is less than the maximum heading change $\Phi_{max}(d)$ given by

$$|\Phi| \leq \Phi_{max}(d) = 2 \cos^{-1} \left(\frac{d_{sep}}{d} \right). \quad (5)$$

Proof: Equation (5) in this corollary follows from (2) in Lemma 2 with the aircraft separation $d_{min} = d$ and heading change $\phi = \phi_{max}(d)$ in Fig. 6(b). ■

Lemma 3 (Diverging/Converging Sequence): Consider a sequence of aircraft (a_k) that diverge along straight lines at point P , e.g., a_i and a_j with $i < j$ in Fig. 8(b). Here, the subscript indicates that aircraft a_j and a_i are separated by at least $(j - i)d$ when the first aircraft a_i is at the divergence point P . Therefore, when the second aircraft a_j is at heading change point P , aircraft a_i would be at a distance $(j - i)d$ from point P . Moreover, as the speed is constant for all aircraft, by the time aircraft a_j moves a distance d_2 from P [see Fig. 8(b)], aircraft a_i also increases its distance to P by d_2 , i.e.,

$$|\phi_k| \leq \phi_{max}(d) = 2 \cos^{-1} \left(\frac{d_{sep}}{d} \right). \quad (6)$$

Moreover, the same conditions are sufficient to avoid conflicts if the directions of the aircraft a_k are reversed and if they are converging at point P , as shown in Fig. 7(b)

Proof: Since the heading change of each aircraft is admissible, from Corollary 2, there are no conflicts between an aircraft that has passed the heading change point P [e.g., a_{k-1} in Fig. 8(a)] and aircraft at or before the heading change point P , e.g., a_k , a_{k+1} , and a_{k+2} in Fig. 8(a).

What needs to be shown is that there is no conflict between two aircraft that have both passed the heading change point P , e.g., a_i and a_j with $i < j$ in Fig. 8(b). Here, the subscript indicates that aircraft a_j and a_i are separated by at least $(j - i)d$ when the first aircraft a_i is at the divergence point P . Therefore, when the second aircraft a_j is at heading change point P , aircraft a_i would be at a distance $(j - i)d$ from point P . Moreover, as the speed is constant for all aircraft, by the time aircraft a_j moves a distance d_2 from P [see Fig. 8(b)], aircraft a_i also increases its distance to P by d_2 , i.e.,

$$d_3 = (j - i)d + d_2. \quad (7)$$

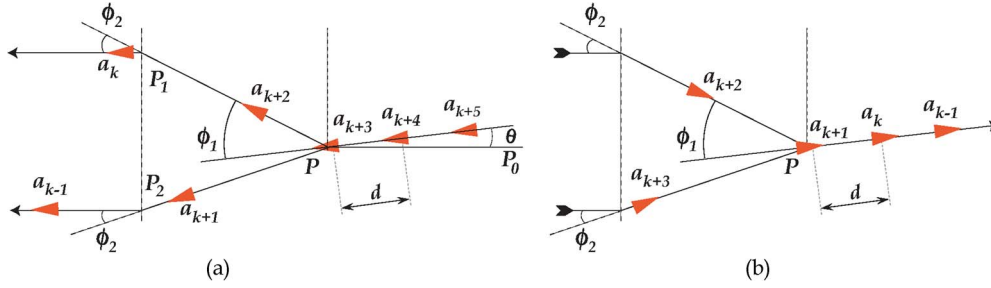


Fig. 9. Two heading changes. (a) Diverging point P followed by a second heading change to achieve a common heading angle for all aircraft. Segment $\overline{PP_0}$ is parallel to the final heading angle after the two heading changes. (b) Converging point P preceded by heading change.

Since the sum of two sides of a triangle is at least the third, from Fig. 8(b), we have

$$d_1 + d_2 \geq d_3. \quad (8)$$

Substituting for d_3 from (7) into (8) yields

$$d_1 + d_2 \geq (j - i)d + d_2 \geq d + d_2 \quad (9)$$

because $i < j$, and therefore

$$d_1 \geq d > d_{\text{sep}} \quad (10)$$

and aircraft that are past the heading change point P also do not have conflicts with each other.

Reversing the directions of the converging aircraft makes it a diverging case, and the lack of conflict follows from the same arguments. ■

In the following lemma, conditions for a conflict-free second heading change following a diverging point (or preceding a converging point) are established.

Lemma 4 (Two Heading Changes): Consider a sequence of aircraft that diverge at point P into two equidistant possible path segments $(\overline{PP_1}, \overline{PP_2})$ followed by a second heading change (at either P_1 or P_2) to achieve a common heading angle for all aircraft, as shown in Fig. 9(a). If the minimal separation of aircraft arriving at waypoint P is $d > d_{\text{sep}}$, then there are no conflicts between the aircraft if the following conditions are met.

- 1) The maximum heading change $\phi_1 < \pi/2$ at P and the heading change $\phi_2 < \pi/2$ (at P_1 and P_2) satisfy the admissible heading change condition [see (5) in Corollary 2], i.e.,

$$|\phi_1| \leq \phi_{\text{max}}(d), \quad |\phi_2| \leq \phi_{\text{max}}(d). \quad (11)$$

- 2) The heading angle difference [see θ in Fig. 9(a)], before and after the two heading changes, is less than $\pi/2$.
- 3) The two heading change points are sufficiently separated, i.e., $d(P, P_1) \geq d_{\text{sep}}$ and $d(P, P_2) \geq d_{\text{sep}}$ in Fig. 9(a).

Moreover, the same conditions are sufficient to avoid conflicts if the flow directions are reversed and if the two heading changes lead to a converging point P , as shown in Fig. 9(b).

Proof: In the following, the lack of conflicts between aircraft for the diverging case [see Fig. 9(a)] is proved. Reversing the directions of the aircraft in the converging case [see Fig. 9(b)] makes it equivalent to the diverging case. Therefore, the lack of conflicts would follow from the same arguments.

There is no conflict between aircraft before the second heading change [at P_1 and P_2 in Fig. 9(a)] because the initial heading-change condition (11) meets the diverging/converging requirement (6) in Lemma 3. Moreover, aircraft before and after the two heading changes are sufficiently separated from each other to avoid conflicts before and after the two heading changes. This is because the closest distance between aircraft before and after the two heading changes is either $d(P, P_1)$ or $d(P, P_2)$ since the overall heading change is less than $\pi/2$ from the second condition of the current lemma; each of these distances ($d(P, P_1), d(P, P_2)$) is at least d_{sep} according to the third condition of the current lemma.

The issue is to show that there is no conflict between any two aircraft when both of them have made the first heading change (at P) and at least one of them has also made the second heading change (at P_1, P_2). Towards this, two cases are considered: 1) aircraft on the same path and 2) aircraft on different paths.

In the first case, aircraft on the same path are separated by d after the second heading change (P_1 or P_2). Therefore, reversing the flow yields an acceptable heading change at P_1 or P_2 by Lemma 2, with no conflicts until P (with the reversed flow). Thus, there are no conflicts due to the second heading change, e.g., between a_k and a_{k+2} in Fig. 9(a).

In the second case, conflicts need to be ruled out between aircraft on different paths, e.g., between a_k and a_{k-1} or between a_k and a_{k+1} in Fig. 9(a). Consider the instant when aircraft a_k has just reached P_1 , as shown in Fig. 10. At this instant, the distance component d_0 (along the aircraft's heading angle) is at least the minimal spacing $d > d_{\text{sep}}$ between aircraft arriving at P because the path segments $(\overline{PP_1}, \overline{PP_2})$ are equidistant. Therefore, there is no conflict between aircraft a_k and aircraft a_{k-1} (which has already made the second heading change) since they are separated by at least d at this time instant. This distance does not change when the two aircraft a_k and a_{k-1} are on parallel paths, and hence, there are no future conflicts as well.

Finally, consider the potential for conflict between aircraft a_k and a_{k+1} , which have not yet made the second heading change, as shown in Fig. 10. The distance d_1 between these two aircraft is at least the minimal spacing $d > d_{\text{sep}}$ of aircraft arriving at P , as shown in the proof of Lemma 3 [see (10)] at this time instant. This conflict-free condition is maintained until aircraft a_{k+1} reaches P_2 because aircraft a_{k+1} is headed away from aircraft a_k until then. It was already shown that there can be no conflicts after aircraft a_{k+1} makes the second heading change—this completes the proof. ■

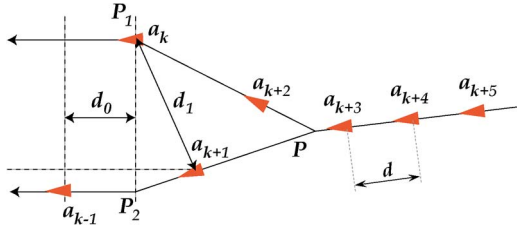


Fig. 10. Separation of aircraft a_k at the second heading change point from aircraft that has (aircraft a_{k-1}) and has not (aircraft a_{k+1}) made the second heading change.

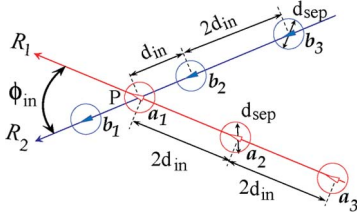


Fig. 11. Intersecting routes. In this example, the aircraft are equally spaced in each route by $2d_{in}$, and the separation at the intersection point is d_{in} .

C. Minimum Aircraft Separation in Intersecting Routes

The following lemma identifies the miles-in-trail separation between aircraft in two intersecting routes to avoid conflict.

Definition 6 (Separation at Intersection Point): Consider the aircraft in two straight-line intersecting routes R_1 and R_2 (as in Fig. 11). The separation at an intersection point is said to be d_{in} if each aircraft at the intersection point (for example, a_1 from route R_1) is at least distance d_{in} from all the other aircraft, e.g., from aircraft b_1 and b_2 on route R_2 in Fig. 11.

Lemma 5 (Minimum Separation at Intersection Point): Consider two straight-line routes R_1 and R_2 with intersection angle $\phi_{in} < \pi$ (the angle between the two departing paths) that does not contain an approaching path), as shown in Fig. 11. Then, the minimum separation d_{in} at the intersection point (see Definition 6), to avoid conflict, is given by

$$d_{in} = \frac{d_{sep}}{\cos(\phi_{in}/2)}. \quad (12)$$

Proof: The movement of aircraft after the intersection can be considered as a heading change with respect to aircraft on the other route. For example, after the intersection point P , the movement of aircraft a_1 on route R_1 (in Fig. 11) can be considered as a heading change ϕ_{in} with respect to route R_2 . Therefore, an aircraft that is at the intersection point P on one route (e.g., a_1 on route R_1) will have no future conflicts (after a_1 departs from point P) with any aircraft on the other route (R_2), provided it is at least d_{in} away from aircraft in the route R_2 , i.e., from Lemma 2 [see (2)], we have

$$d(a_1, b_1) \geq \frac{d_{sep}}{\cos(\phi_{in}/2)} = d_{in}; \quad d(a_1, b_2) \geq d_{in}.$$

This same condition (and argument) is sufficient to show that an aircraft at the intersection point (e.g., a_1 on route R_1) will

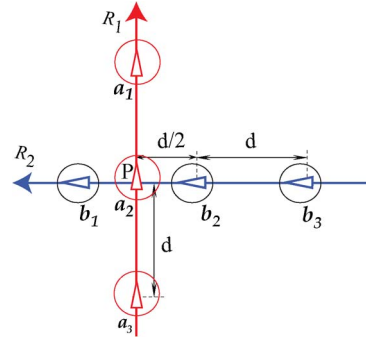


Fig. 12. Intersecting perpendicular routes. Separation between aircraft in each route is d , and the minimum separation at the intersection point (as in Definition 6) is $d/2$.

not have past conflicts (before arrival at point P) with an aircraft on another route (e.g., R_2). In particular, by reversing the direction of the aircraft in the two routes, the previously converging aircraft (before intersection point P) becomes diverging, and therefore, there are no past conflicts under the spacing condition [12] of the current lemma. ■

Corollary 3 (Conflict-Free Perpendicular Intersection): Let the spacing between aircraft in each of the two perpendicularly intersecting routes (R_1, R_2) be d , and let the minimum separation at the intersection point (see Definition 6) be $d/2$, as shown in Fig. 12. Then, there are no conflicts between aircraft in the two routes if

$$d \geq d_{\pi/2} = 2\sqrt{2}d_{sep}. \quad (13)$$

Proof: This follows from Lemma 5 with $\phi_{in} = \pi/2$ and $d_{in} = \sqrt{2}d_{sep}$. ■

D. CRP

In the following, a CRP for two perpendicularly intersecting routes R_1 and R_2 is presented when the minimal spacing between arriving aircraft along each route is at least \underline{d} . Based on the results in Corollary 3, a CRP can be developed for perpendicular intersections provided the separation of aircraft in each route \underline{d} is greater than $d_{\pi/2} = 2\sqrt{2}d_{sep}$. However, in general, aircraft arrival spacing \underline{d} might be less than $d_{\pi/2}$ since a spacing of $d_{sep} < d_{\pi/2}$ is sufficient for safety on a single route. Note that the spacing between aircraft (from a single route) can be increased by splitting the route into multiple paths. For example, splitting the route into three paths can enable the spacing on each path to be increased by three times (i.e., $3\underline{d}$), which is sufficiently large to develop conflict-free perpendicular intersections (from Corollary 3) since

$$3\underline{d} > 3d_{sep} > 2\sqrt{2}d_{sep} = d_{\pi/2}.$$

This motivates the following CRP for perpendicular intersecting routes—it is comprised of four subprocedures: 1) synchronize; 2) diverge; 3) intersect; and 4) converge, as shown in Fig. 13 for route R_1 ; these subprocedures and conditions for avoiding conflicts are subsequently discussed.

1) *Synchronized Arrival:* The synchronization procedure ensures that the scheduled time of arrival (STA) of aircraft at

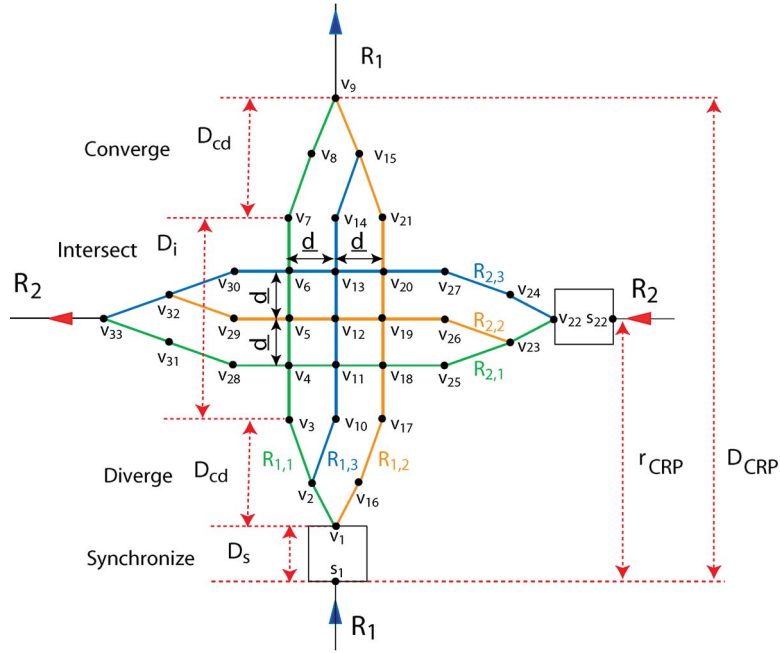


Fig. 13. Overview of actions in the conflict-resolution algorithm. 1) Synchronize; 2) diverge; 3) intersect; and 4) converge. Waypoints v are numbered along paths $R_{1,1}$, $R_{1,3}$, and $R_{1,2}$ for route R_1 and then along the paths for route R_2 (from left to right and from bottom to top).

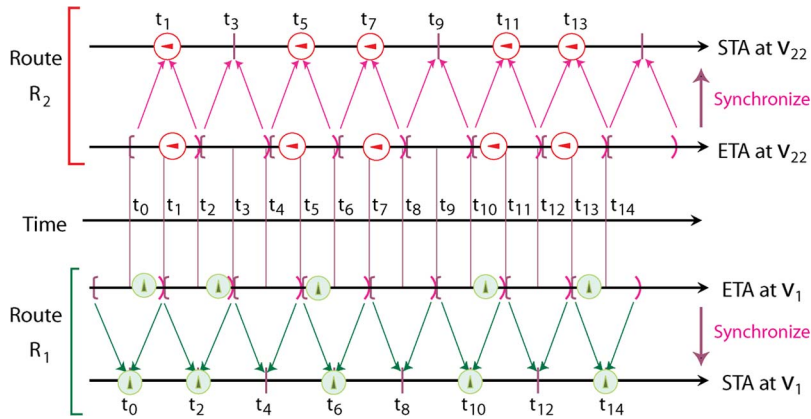


Fig. 14. Assignment of STA at the start of the diverge procedure, for each route, based on the expected time of arrival (ETA) of each aircraft.

the initial waypoints (v_1 for route R_1 and v_{22} for route R_2 in Fig. 13) is at discrete time instants t_k , i.e.,

$$t_k = k \left(\frac{d/2}{v_{sp}} \right) = kT_{d/2} \quad (14)$$

where k is a nonnegative even integer for route R_1 and a nonnegative odd integer for route R_2 .

Remark 10: The time difference, i.e., $2T_{d/2}$ in (14), between two scheduled $STAs$ on a single route corresponds to the time needed to travel (with nominal speed v_{sp}) the minimum separation distance d between aircraft arriving in each route.

Definition 7 (ETA and STA for Synchronization): Given an expected arrival time (ETA) t at the initial waypoints of the diverge procedure (v_1 or v_{22} in Fig. 13), the synchronization procedure assigns an STA t_k to the initial waypoint, as shown in Fig. 14. In particular, the STA t_k is chosen to be the closest (and smallest) discrete time instant to ETA t with an even integer k

for route R_1 and an odd integer k for route R_2 , i.e., for any integer k

$$\begin{aligned} \text{ETA at } V_1 \in [t_{2k+1}, t_{2k+3}) &\rightarrow \text{STA} = t_{2k+2} \\ \text{ETA at } V_{22} \in [t_{2k}, t_{2k+2}) &\rightarrow \text{STA} = t_{2k+1}. \end{aligned} \quad (15)$$

Remark 11: As seen in Fig. 14, the potential $STAs$ are separated by two discretized time points t_k defined in (14). Therefore, during synchronization, the arrival time only needs to be adjusted by a maximum of $T_{d/2}$ [which is defined in (14)]. Towards this arrival time adjustment, the distance traveled by an aircraft needs to be changed by a maximum of $\pm d/2$ from the nominal travel distance during synchronization.

The following synchronization procedure achieves the STA by using offset maneuvers. The nominal path length (between node s_1 to node v_1 on route R_1 or between node s_{22} to node v_{22} on route R_2 in Fig. 13) is changed by δ_x , where

$$\delta_x = (STA - ETA)v_{sp}. \quad (16)$$

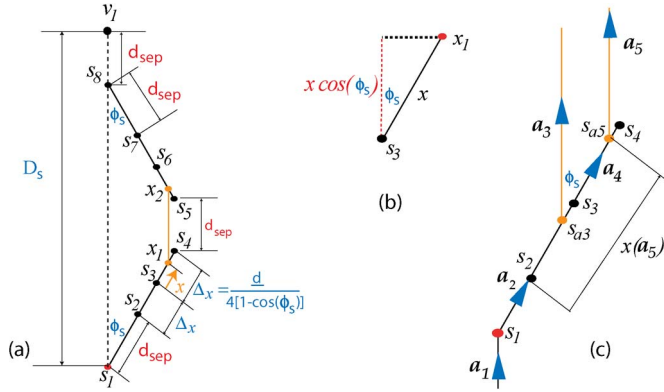


Fig. 15. (a) Synchronization procedure for route R_1 . Distance x between waypoints s_3 and x_1 is given by (18). The maximum value Δx of x corresponds to $\delta_x = \underline{d}/2$ in (18). (b) Increase in path length due to x . (c) Zoom view of possible conflict between aircraft a_j for $j = 1$ to 5.

The offset procedure for synchronization is subsequently described for route R_1 ; the procedure is similar for route R_2 and is omitted here for brevity.

Remark 12: Path extension procedures to adjust STAs are currently used in ATC, for example, to meter and space the aircraft arrival at airport runways, e.g., [9], [36], and [37].

Lemma 6 (Conflict-Free Synchronization): Given a desired change in path length $|\delta_x| \leq \underline{d}/2$ [see (16)], the synchronization procedure shown in Fig. 15(a) is conflict free if

- 1) the initial heading change angle

$$0 < \phi_s < \pi/2 \quad (17)$$

satisfies the admissible heading change condition [see (5) in Corollary 2];

- 2) the distance x from waypoint s_3 [in Fig. 15(a)] to the second heading change at x_1 is given by

$$x = \frac{\delta_x}{2[1 - \cos(\phi_s)]}. \quad (18)$$

Proof: The increase in path length by changing the second heading change waypoint by x (from s_3 to x_1) is given by $x[1 - \cos(\phi_s)]$, as seen in Fig. 15(b). Since there are two such path-length increases [between s_3 and x_1 and between x_2 and s_6 in Fig. 15(a)], the total path change when compared with the nominal path (with $\delta_x = 0$, $x = 0$ and the second heading change at waypoint s_3) is equal to the desired change in path length δ_x from (18). Thus, the synchronization procedure [with δ_x from (16)] achieves the time difference between STA and ETA at waypoint v_1 .

Two cases are considered to show that there are no conflicts during synchronization: 1) when the path changes δ_x are the same for two aircraft and 2) when the path changes δ_x are different for two aircraft. For each case, it is sufficient to show that there are no conflicts before the third heading change on segment $\overline{s_5 s_8}$ because, by symmetry, reversing the flow would lead to no conflicts until segment $\overline{s_1 s_4}$ with aircrafts arriving at s_8 with minimal spacing \underline{d} .

For aircraft with the same path change (i.e., same x), there are no conflicts because the heading changes ϕ_s along a single path [e.g., path $\{s_1, x_1, x_2, s_8, v_1\}$ shown in Fig. 15(a)] satisfy

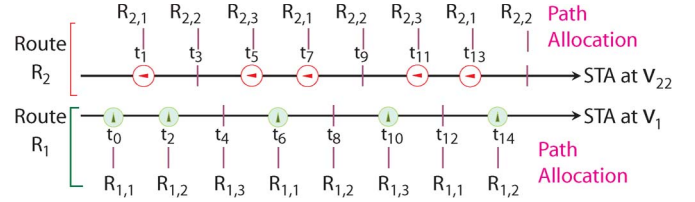


Fig. 16. Path allocation. Each aircraft is assigned a path based on its STA.

the conditions of Lemma 4. For the same reason, there are no conflicts between aircraft a_1, a_2 , and a_3 (and similarly between aircraft a_1, a_2, a_4, a_5) in Fig. 15(c), which represents the case with two different path changes, i.e., different x .

The issue is to show that there are no conflicts between aircraft that are not within the purview of the two heading changes in Lemma 4, e.g., between aircraft a_3 and a_4 or aircraft a_3 and a_5 . Aircraft a_3 and a_4 were separated by at least \underline{d} when the one closest to waypoint s_{a3} was at s_{a3} ; therefore, a_3 and a_4 do not have a conflict since the divergence angle ϕ_s at s_{a3} is an admissible heading change (condition 1 of the current lemma). Finally, the paths of a_3 and a_5 are parallel after the second heading change (and before the third heading change); therefore, a_3 and a_5 are conflict free because there was no conflict (from previous arguments) when the aircraft closest to segment $\overline{s_1 s_4}$ was just leaving segment $\overline{s_1 s_4}$, i.e., at either s_{a3} or s_{a5} . ■

2) *Path Assignment in CRP:* The CRP consists of splitting each route (R_1, R_2) into three paths and choosing one of the paths for each arriving aircraft. In particular, the three paths $\{R_{1,i}\}_{i=1}^3$ for route R_1 (shown in Fig. 13) are described by the following set of waypoints (v_i):

$$\begin{aligned} R_{1,1} &= \{v_1, v_2, v_3, v_4, v_5, v_6, v_7, v_8, v_9\} \\ R_{1,2} &= \{v_1, v_{16}, v_{17}, v_{18}, v_{19}, v_{20}, v_{21}, v_{15}, v_9\} \\ R_{1,3} &= \{v_1, v_2, v_{10}, v_{11}, v_{12}, v_{13}, v_{14}, v_{15}, v_9\} \end{aligned} \quad (19)$$

and the three paths $\{R_{2,i}\}_{i=1}^3$ for route R_2 are

$$\begin{aligned} R_{2,1} &= \{v_{22}, v_{23}, v_{25}, v_{18}, v_{11}, v_4, v_{28}, v_{31}, v_{33}\} \\ R_{2,2} &= \{v_{22}, v_{23}, v_{26}, v_{19}, v_{12}, v_5, v_{29}, v_{32}, v_{33}\} \\ R_{2,3} &= \{v_{22}, v_{24}, v_{27}, v_{20}, v_{13}, v_6, v_{30}, v_{32}, v_{33}\}. \end{aligned} \quad (20)$$

The path assignment procedure is illustrated in Fig. 16; the procedure is based on the index k in the STA t_k at the initial waypoints (v_1 or v_{22}).

Definition 8 (Path Allocation Procedure): Without loss of generality, it is assumed that aircraft do not arrive before time t_0 . If the STA k is even (i.e., aircraft on route R_1 arriving at waypoint v_1), then assign path $R_{1,j+1}$, where j is $k/2$ modulus 3. If k is odd (route R_2 at waypoint v_{22}), then assign path $R_{2,j+1}$, where j is $(k-1)/2$ modulus 3, as illustrated in Fig. 16.

Remark 13: The path allocation rule is cyclic and repeats after every six discrete time instants.

3) *Conflict-Free Intersect Subprocedure:* The following lemma shows that the splitting of each route into three paths allows for a conflict-free intersection.

Lemma 7 (Intersection is Conflict Free): Aircraft that arrive synchronized (see Definition 7) have no conflicts with each

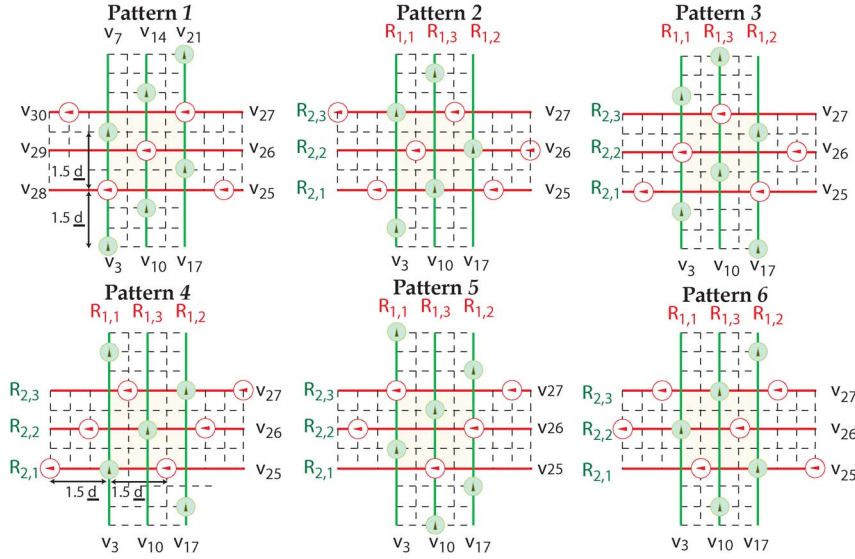


Fig. 17. All possible positions of aircraft whenever an aircraft arrives at a start of the straight line segment of the intersection in Fig. 13. Some of the positions might be empty, i.e., not have an aircraft; however, aircraft cannot occupy another location due to (a) arrival synchronization and (b) equidistant path lengths to the straight line segments from the arrival points v_1 and v_{22} .

other in the intersection area (marked by D_i in Fig. 13 for Route R_1) with the use of the path assignment procedure in Definition 8 if the path lengths from the arrival points to the beginning of the straight line segments (e.g., from v_1 to v_3 or from v_{22} to v_{26} in Fig. 13) are all equal, then all possible positions of other aircraft, whenever an aircraft enters a straight line segment, are shown in Fig. 17. Some of the potential aircraft positions (at the discrete time instants) shown in Fig. 17 may be empty, i.e., they might not have an aircraft; however, aircraft cannot occupy any other location due to 1) arrival synchronization and 2) equidistant path lengths to the straight line segments from arrival points v_1 and v_{22} . Aircraft in perpendicular paths (for example, $R_{1,1}$ and $R_{2,1}$ in Fig. 17) do not have conflicts since the conditions of Corollary 3 are satisfied. In particular, even when all the aircraft are present, the separation between aircraft D in each path is $D = 3d > 3d_{sep}$, and the separation at the intersection point is $D/2 = 1.5d$ (see patterns 1 and 4 in Fig. 17). There are no conflicts between aircraft on parallel paths because the paths are separated by $d > d_{sep}$. ■

Proof: If the path lengths from the arrival points to the beginning of the straight line segments (e.g., from v_1 to v_3 or from v_{22} to v_{26} in Fig. 13) are all equal, then all possible positions of other aircraft, whenever an aircraft enters a straight line segment, are shown in Fig. 17. Some of the potential aircraft positions (at the discrete time instants) shown in Fig. 17 may be empty, i.e., they might not have an aircraft; however, aircraft cannot occupy any other location due to 1) arrival synchronization and 2) equidistant path lengths to the straight line segments from arrival points v_1 and v_{22} . Aircraft in perpendicular paths (for example, $R_{1,1}$ and $R_{2,1}$ in Fig. 17) do not have conflicts since the conditions of Corollary 3 are satisfied. In particular, even when all the aircraft are present, the separation between aircraft D in each path is $D = 3d > 3d_{sep}$, and the separation at the intersection point is $D/2 = 1.5d$ (see patterns 1 and 4 in Fig. 17). There are no conflicts between aircraft on parallel paths because the paths are separated by $d > d_{sep}$. ■

4) *Diverge/Converge Subprocedures Without Conflict:* The diverge and converge procedures separate and merge the routes 1) without conflicts and 2) while preserving synchronization in the different paths (for conflict avoidance at the intersection, see Lemma 7) by using equal-length maneuvers, as shown in Fig. 18. For example, for path $R_{1,1}$, the length from v_1 to v_3 is the same as the length for path $R_{1,3}$ from v_1 to v_{10} via v_2 in Fig. 18(a). There are no conflicts during these procedures if the maximum heading change in the procedures (e.g., ϕ_{cd} in Fig. 18) is small, as shown for route R_1 . The same result holds for route R_2 .

Lemma 8 (Conflict-Free Diverge/Converge): Aircraft that arrive synchronized and with minimal separation of d (see Definition 7) do not have conflicts after the arrival points (v_1 , v_{22} in Fig. 13) with the use of the path assignment procedure

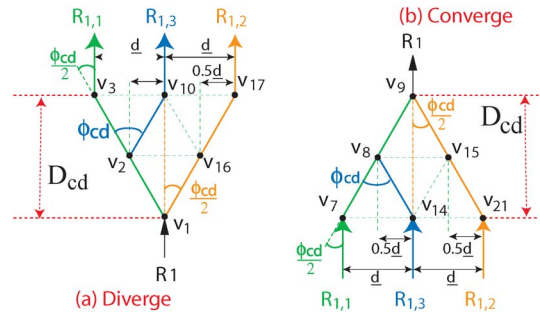


Fig. 18. Converge and diverge procedures for route R_1 using equal-length path segments. (a) Diverge. (b) Converge.

in Definition 8 and the diverge/converge procedures in Fig. 18, provided the following two conditions are satisfied.

- 1) The maximum heading change $0 < \phi_{cd}$ during the diverge/converge procedures satisfies the admissible heading change condition when the aircraft have an initial separation of at least d [(5) in Corollary 2], i.e.,

$$|\phi_{cd}| \leq \phi_{\max}(d) = 2 \cos^{-1} \left(\frac{d_{sep}}{d} \right). \quad (21)$$

- 2) The maximum heading change $0 < \phi_{cd}$ is sufficiently small to ensure that two sequential heading changes are well separated from each other to avoid conflicts due to multiple heading changes, i.e.,

$$D_{cd} = \frac{d}{\tan(\phi_{cd}/2)} \geq 2d_{sep}. \quad (22)$$

Proof: The proof for the converge procedure follows by considering the diverge procedure with the aircraft directions reversed. Therefore, it is sufficient to show the lack of conflict in the diverge procedure.

The lack of conflict between aircraft due to the first diverge procedure (at v_1), before the second heading change, follows

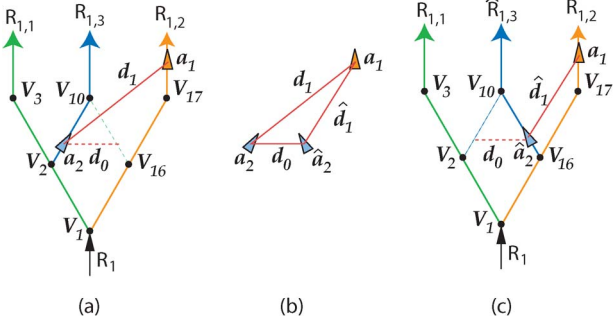


Fig. 19. Paths $R_{1,2}$ and $R_{1,3}$ do not have conflicts because there are no conflicts between paths $R_{1,2}$ and $\hat{R}_{1,3}$.

from Lemma 3 and condition 1 [see (21)] of the current lemma. Aircraft after the second heading change (at v_2, v_{16}) do not conflict with aircraft before the first heading change (at v_1) because they are sufficiently separated (by d_{sep}) because of the second condition [see (22)] of the current Lemma. Therefore, the following proof only needs to consider the aircraft after the first heading change.

Paths $R_{1,1}$ and $R_{1,3}$, in Fig. 18(a), have no conflicts because the conditions of the current lemma satisfy the conditions of the two-heading-change Lemma 4; similarly, there are no conflicts between paths $R_{1,1}$ and $R_{1,2}$ by the same argument. However, paths $R_{1,2}$ and $R_{1,3}$ do not match the formulation of the two-heading-change Lemma 4. To obtain a match, the path $R_{1,3}$ in which aircraft move from v_1 to v_{10} via v_2 should be changed to a path $\hat{R}_{1,3}$ in which aircraft move from v_1 to v_{10} via v_{16} —e.g., aircraft a_2 on $R_{1,3}$ in Fig. 19(a) would be at position \hat{a}_2 on $\hat{R}_{1,3}$, as shown in Fig. 19(c). Then, the absence of conflict between paths $R_{1,2}$ and $\hat{R}_{1,3}$ can be shown using the two-heading-change Lemma 4. Therefore, the distance \hat{d}_1 between aircraft \hat{a}_2 and a_1 is greater than the minimum spacing d_{sep} in Fig. 19(c).

The results of the current lemma follow since the distance of an aircraft (e.g., a_1) on $R_{1,2}$ to an aircraft on $R_{1,3}$ [e.g., distance d_1 to aircraft a_2 in Fig. 19(a)] is always greater than the distance to a corresponding aircraft on $\hat{R}_{1,3}$ [e.g., distance \hat{d}_1 to aircraft $\hat{a}_2 > d_{\text{sep}}$ in Fig. 19(c)] by the triangle inequality, as illustrated in Fig. 19(b), because $d_1 \geq \hat{d}_1 + d_0 \geq \hat{d}_1 > d_{\text{sep}}$. ■

5) *Spatial and Temporal Bounds on CRP*: The perpendicular CRP described in this section is bounded both spatially and temporally.

Lemma 9 (Bounds on CRP): The CRP, described in Section III-D and illustrated in Fig. 13, is bounded spatially and temporally.

Proof: The spatial distance D_{CRP} between the waypoint s_1 before synchronization and the last waypoint v_9 after the converge in Fig. 13 is the sum of 1) the distance for synchronization $D_s = d(s_1, v_1)$ in Fig. 15 given by

$$\begin{aligned} D_s &= 2d_{\text{sep}} + [2d_{\text{sep}} + 4\Delta_x] \cos(\phi_s) \\ &= 2d_{\text{sep}} [1 + \cos(\phi_s)] + \frac{d \cos(\phi_s)}{1 - \cos(\phi_s)} \end{aligned} \quad (23)$$

2) the distance for converge $D_{\text{cd}} = d(v_1, v_{10})$ in Fig. 18, which is given by (22); 3) the distance for the intersection

$D_i = d(v_{10}, v_{14})$ in Fig. 17 (see pattern 1) given by

$$D_i = 5\hat{d} \quad (24)$$

and 4) the distance for the converge $D_{\text{cd}} = d(v_{14}, v_9)$ in Fig. 18, which is the same as the distance for the diverge. Thus, the spatial distance D_{CRP} for the CRP (see Fig. 13) given by

$$\begin{aligned} D_{\text{CRP}} &= D_s + 2D_{\text{cd}} + D_i \\ &= 2d_{\text{sep}} [1 + \cos(\phi_s)] + \frac{d \cos(\phi_s)}{1 - \cos(\phi_s)} + \frac{2\hat{d}}{\tan(\phi_{\text{cd}}/2)} + 5\hat{d} \end{aligned} \quad (25)$$

is bounded since $0 < \phi_s < \pi/2$ from (17) in Lemma 6 and $0 < \phi_{\text{cd}}$ from Lemma 8.

Similarly, the path length P_{CRP} for any aircraft on route R_1 between waypoint s_1 before synchronization and the last waypoint v_9 after converge in Fig. 13 is less than the sum of the maximum path length for synchronization P_s between s_1 and v_1 in Fig. 15 given by

$$\begin{aligned} P_s &= 4d_{\text{sep}} + 4\Delta_x \\ &= 4d_{\text{sep}} + \frac{d}{1 - \cos(\phi_s)} \end{aligned} \quad (26)$$

the path length for converge P_{cd} between v_1 and v_{10} in Fig. 18 given by

$$P_{\text{cd}} = \frac{d}{\sin(\phi_{\text{cd}}/2)} \quad (27)$$

the path length for the intersection P_i between v_{10} and v_{14} in Fig. 17 (see pattern 1) given by

$$P_i = 5\hat{d} \quad (28)$$

and the path length for the converge P_{cd} between v_{14} and v_9 in Fig. 18, which is the same as the path length for the diverge [in (27)]. Thus, the maximum path length P_{CRP} for the CRP given by [from (26)–(28)]

$$\begin{aligned} P_{\text{CRP}} &= P_s + 2P_{\text{cd}} + P_i \\ &= 4d_{\text{sep}} + \frac{d}{1 - \cos(\phi_s)} + \frac{2\hat{d}}{\sin(\phi_{\text{cd}}/2)} + 5\hat{d} \end{aligned} \quad (29)$$

is bounded since $0 < \phi_s < \pi/2$ from (17) in Lemma 6, and $0 < \phi_{\text{cd}}$ from Lemma 8.

Therefore, the temporal length (i.e., the maximum time T_{CRP} needed from s_1 to v_9 in Fig. 13) is bounded and given by

$$T_{\text{CRP}} = \frac{P_{\text{CRP}}}{v_{\text{sp}}} \quad (30)$$

where v_{sp} is the nominal speed, and the maximum path length is P_{CRP} from (29). ■

Corollary 4: The distance r_{CRP} , from the start of the synchronization (e.g., at s_1) to the intersection of the two routes at v_{12} in Fig. 13, is finite.

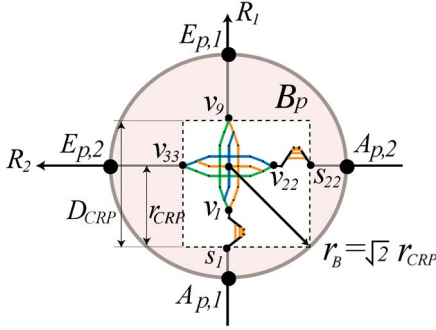


Fig. 20. Size of the conflict-resolution disc, as discussed in Fig. 5, for the perpendicular CRP.

Proof: From Fig. 13 and (25), we have

$$\begin{aligned} r_{\text{CRP}} &= D_s + D_{\text{cd}} + D_i/2 \\ &= 2d_{\text{sep}} [1 + \cos(\phi_s)] + \frac{d \cos(\phi_s)}{1 - \cos(\phi_s)} + \frac{d}{\tan(\phi_{\text{cd}}/2)} + 2.5d. \end{aligned} \quad (31)$$

Again, as in the proof of Lemma 9, r_{CRP} is bounded since $\phi_s < \pi/2$ from Lemma 6 and $0 < \phi_{\text{cd}}$ from Lemma 8. ■

6) *CRP Satisfies Decoupling Conditions:* The perpendicular CRP satisfies the decoupling conditions of Lemma 1, as subsequently shown.

Lemma 10 (CRP is Decoupling): The perpendicular CRP (Section III-D) is a decoupling perpendicular CRP (where each conflict region L_p has radius $r_p = d_{\text{sep}}$, as in Definition 5) under the following two conditions.

- 1) The intersecting routes R_1 and R_2 are straight-line perpendicularly intersecting segments in the conflict-resolution disc B_p (see Figs. 5 and 20), i.e., for a distance

$$r_B = \sqrt{2} r_{\text{CRP}} \quad (32)$$

from the intersection of the two routes R_1 and R_2 at waypoint v_{12} (see Fig. 13) with r_{CRP} , as in (31).

- 2) The airspace is κ -sparse (see Definition 2) with

$$\kappa = \frac{r_B}{d_{\text{sep}}} = \frac{\sqrt{2} r_{\text{CRP}}}{d_{\text{sep}}}. \quad (33)$$

Proof: The conflict-resolution disc B_p circumscribes the CRP, as illustrated in Fig. 20, since the farthest waypoint of the CRP from the center v_{12} is the arrival point for the synchronization procedure, e.g., s_1 for route R_1 in Fig. 13. Note that the aircraft in the perpendicular CRP in Fig. 13 has no conflict with aircraft in other routes in the airspace by condition 2 of this lemma (see Definition 2). What remains to be shown is that the perpendicular CRP in Fig. 13 satisfies all the conditions of Lemma 1: intent, liveness, fairness, and exit spacing.

Local Intent: The paths for each route end at the same point on the original route, e.g., at waypoint v_9 on route R_1 in Fig. 13. Moreover, the arrival points $A_{p,1}$ and $A_{p,2}$ and the exit points $E_{p,1}$ and $E_{p,2}$ at the boundary of the disc B_p (see Fig. 20) lie on routes R_1 and R_2 due to Condition 1 of this lemma. Therefore, the CRP satisfies the local intent condition of exiting along the desired route.

Local Liveness: The maximum path length P_{max} in the conflict-resolution disc B_p is given by (from (25), (29), (32), and Fig. 20)

$$\begin{aligned} P_{\text{max}} &= (2r_B - D_{\text{CRP}}) + P_{\text{CRP}} \\ &= (2\sqrt{2} r_{\text{CRP}} - D_{\text{CRP}}) + P_{\text{CRP}} \end{aligned} \quad (34)$$

which is bounded by Lemma 9 and Corollary 4. Therefore, the time needed for any aircraft to pass through the CRP is bounded by

$$T_{\text{max}} = P_{\text{max}}/v_{\text{sp}} \quad (35)$$

and thus, the local liveness condition is satisfied.

Local Fairness: The aircraft keep the same arrival sequence in the synchronization procedure (see Fig. 14), and all the path lengths are the same after the synchronization—therefore, aircraft exit the conflict disc B_p (in each route) with the same sequence as the arrival at B_p . Therefore, the CRP meets the local FCFS fairness requirement.

Exit Spacing: After synchronization, the arrival time at the diverge point (e.g., v_1 for route R_1) is at least separated by $2T_{d/2}$ in each route, which also corresponds to the minimal time between exiting aircraft at the final point of the conflict disc (since the path lengths are the same after the diverge point). This minimum time $2T_{d/2}$, between aircraft exiting along each route, corresponds to the required minimal spacing of d at the exit (see Remark 10). ■

Corollary 5 (CRP Without Flow-Level Reduction): Reductions in aircraft flow levels are not needed to resolve en-route conflicts for intersecting routes with the proposed CRP under conditions of Lemma 10.

Proof: This follows from Lemma 10, because each local CRP is guaranteed to maintain an exit spacing of d , provided the minimal arrival spacing is $d > d_{\text{sep}}$. ■

Remark 14: The size of the conflict-resolution disc B_p (in Fig. 20) depends on the aircraft spacing d used in the CRP, as seen in (31) and (32). However, because of the synchronization procedure, it is acceptable to choose the distance d (in the design of the CRP) to be smaller than the expected minimal aircraft spacing d^* , i.e.,

$$d_{\text{sep}} < d \leq d^*$$

if the expected minimal aircraft spacing d^* is large.

IV. DISCUSSION OF IMPLEMENTATION ISSUES

This paper demonstrated the existence of decoupled CRPs when the airspace conflicts consist of perpendicular intersection. Future work should consider implementation issues such as nonperpendicular intersections and uncertainties (e.g., in the aircraft speed). These issues are briefly discussed as follows.

A. Nonperpendicular Intersections

If the intersection angle between the routes are not perpendicular, then the routes could be reoriented to make perpendicular intersection or the CRPs could be developed for nonperpendicular intersections.

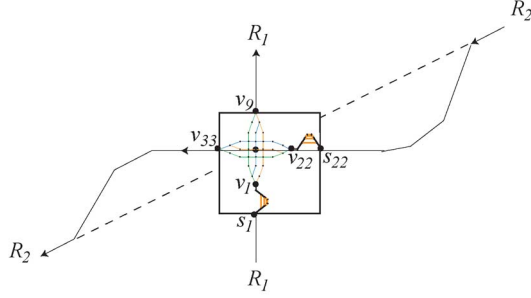


Fig. 21. Example reorientation of a route R_2 with four heading changes to enable the use of the perpendicular CRP.

1) *Indirect Solution by Reorienting Routes*: The routes could be reoriented to generate a perpendicular intersection, e.g., route R_2 is reoriented in Fig. 21. Note that each heading change in the reorientation procedure should be less than the maximum admissible heading change ϕ_{\max} (see (5) in Corollary 2) for the route to be reoriented. Therefore, the minimum number N_r of heading changes needed for reorientation before arriving at the perpendicular CRP (e.g., s_{22} in Fig. 21) is the smallest integer that satisfies

$$[N_r - 1]\phi_{\max} > \phi_R. \quad (36)$$

With such a reorientation, the size of the conflict-resolution disc (B_p in Fig. 20) needs to be increased to include the reorientation procedure; therefore, the conflicts have to be more sparse to ensure that the CRP does not generate additional conflicts due to the reorientation procedure.

2) *Direct Solution for Nonperpendicular Case*: An alternate approach is to use nonperpendicular intersections of the paths in the CRP, i.e., in Fig. 17. The number of paths into which each route needs to be split, with nonperpendicular intersections, can be determined by the minimal spacing d_{in} for conflict-free intersection in Lemma 5 and the minimum arrival spacing along each route \underline{d} . The CRP developed in the previous section could then be extended for nonperpendicular intersections using similar subprocedures of synchronize, diverge, intersect, and converge, as in Fig. 13.

Remark 15: If the spacing between aircraft is substantially different along the two intersecting routes, then the number of paths into which each route needs to split to generate sufficient space between aircraft for conflict-free intersection can be different. For example, the number of paths needed for one of the routes could be two or even one instead of the three paths shown in Fig. 13.

B. Robustness to Arrival Time and Speed Uncertainties

The CRP can be made locally robust (with no conflicts in the conflict-resolution disc B_p) in the presence of deviations in the arrival time (δ_{STA}) and the nominal speed (δ_v) by designing the CRP with a larger minimal separation distance $\bar{d}_{\text{sep}} > d_{\text{sep}}$ between aircraft. In particular, the uncertainty E_p in the aircraft position, in the conflict disc, is bounded by

$$E_p = |\delta_{\text{STA}}|v_a + T_v|\delta_v| \quad (37)$$

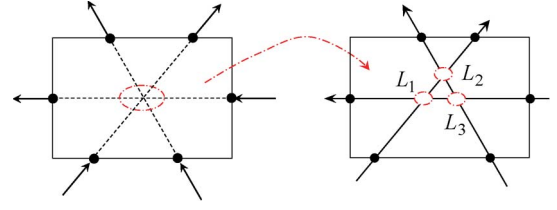


Fig. 22. Compound intersection of multiple routes can be rearranged into a set of simple intersections, each with two routes.

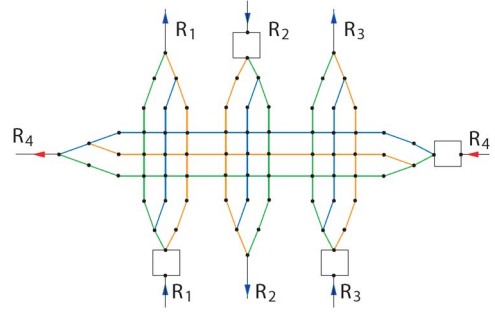


Fig. 23. Achieving multiple intersections along route R_4 before the converge procedure can reduce the space needed for the CRP.

where $T_v = P_{\max}/v_a$ is the maximum time needed to transit through the conflict-resolution disc [as in (35)], and v_a is the speed of the aircraft. Due to this uncertainty, the closest aircraft spacing (within the conflict disc) is reduced from the nominally guaranteed value of \bar{d}_{sep} to $\bar{d}_{\text{sep}} - 2|E_{\max}|$, where the maximum uncertainty $|E_{\max}|$ in aircraft position can be bounded by

$$|E_{\max}| \leq |\Delta_{\text{STA}}|(v_{sp} + \Delta_v) + \frac{P_{\max}}{v_{sp} - \Delta_v}|\Delta_v| \quad (38)$$

where $|\Delta_{\text{STA}}|$ is the maximum deviation in the arrival time at the conflict disc, and $|\Delta_v| < v_{sp}$ is the maximum deviation in the speed. Therefore, there are no conflicts within the CRP's conflict-resolution disc B_p provided the maximum deviations in the speed $|\Delta_v|$ and arrival time $|\Delta_{\text{STA}}|$ are sufficiently small, i.e.,

$$2|E_{\max}| \leq \bar{d}_{\text{sep}} - d_{\text{sep}}. \quad (39)$$

C. Multiple Close Intersections

Compound conflicts (e.g., multiple intersections in close proximity, as studied in [22]) are not considered in the CRP design presented in this paper; however, the routes could be redefined so that such compound conflicts can be considered as a set of simple conflicts, as studied in, e.g., [38] and illustrated in Fig. 22. Resolution of conflicts at each of these simple intersections can be addressed using the CRP developed in this paper.

When multiple conflicts occur in close proximity, the space needed for the CRP could be reduced by completing more than one intersection before the converge procedure, e.g., as illustrated in Fig. 23. Moreover, the synchronize, diverge, and merge procedures (proposed in this paper) could be combined with offset-type procedures for the intersections [22], [25].

D. Ameliorating the Assumptions

Assumptions such as constant speed and instantaneous turns could be ameliorated in future work. However, the main concept to achieve decoupled decentralized CRPs, i.e., splitting of the main route into sufficient number of equal-length paths to enable route intersections without reducing the flow levels, would still be valid.

The constant speed assumption is used in each local conflict-resolution algorithm (in Fig. 13). It is possible to consider different speeds for aircraft in different conflict regions (with the same speed in each conflict region), which would require procedures (such as overtake protocols) to manage the flow of aircraft outside the intersection-based conflict regions. Additionally, while the current conflict-resolution algorithm is robust to small variations in aircraft speed in each conflict-resolution region (see Section IV-B), the proposed CRP could be generalized to handle intersecting routes with different speeds. The main concepts of the current CRP would be applicable to generalized procedures, such as the need 1) to split each route into multiple paths with sufficient spacing to enable conflict-free intersections and 2) to synchronize the arrivals.

The instantaneous turns, which were used in the merge and diverge procedures associated with splitting the route into multiple paths (in Fig. 13), can be generalized to include the effects of aircraft turn dynamics. This would necessitate, for example, the consideration of continuous turns instead of instantaneous turns, particularly in the merge and diverge portions of the proposed CRP. The effect of such continuous turns on decoupling CRP design is studied in our recent work [39], which quantifies the arrival spacing conditions with the inclusion of aircraft turn dynamics.

V. CONCLUSION

This paper has addressed the design of provably-safe decentralized CRPs. In particular, necessary and sufficient conditions to decouple CRPs in intersecting routes were identified. Additionally, decentralized en-route CRPs were identified, which satisfied the decoupling conditions for each local conflict and thereby enabled global conflict resolution.

REFERENCES

- [1] G. Chatterji, B. Shridar, and K. Bilimoria, "En-route flight trajectory prediction for conflict avoidance and traffic management," in *Proc. AIAA Guid., Navigat., Control Conf.*, San Diego, CA, Jul. 29–31, 1996, pp. 1–11.
- [2] W. B. Cotton, "Formulation of the air traffic system as a management problem," *IEEE Trans. Commun.*, vol. COM-21, no. 5, pp. 375–382, May 1973.
- [3] K. D. Bilimoria, K. S. Seth, H. Q. Lee, and S. R. Grabbe, "Performance evaluation of airborne separation assurance for free flight," in *Proc. AIAA Guid., Navigat., Control Conf.*, Denver, CO, Aug. 14–17, 2000, pp. 1–9.
- [4] A. Mukherjee and M. Hansen, "A dynamic rerouting model for air traffic flow management," *Transp. Res. Part B*, vol. 43, no. 1, pp. 159–171, Jan. 2009.
- [5] D. Bertsimas and S. Stock-Patterson, "The air traffic flow management with en route capacities," *Oper. Res.*, vol. 46, no. 3, pp. 406–422, 1998.
- [6] B. Sridhar, S. R. Grabbe, and A. Mukherjee, "Modeling and optimization in traffic flow management," *Proc. IEEE*, vol. 96, no. 12, pp. 2060–2080, Dec. 2008.
- [7] K. R. Allendoerfer and R. Weber, "Playmaker: An application of case-based reasoning to air traffic control plays," in *Proc. 7th ECCBR*, Madrid, Spain, Aug. 30–Sep. 2, 2004, vol. 3155, pp. 476–488.
- [8] Y. Wan and S. Roy, "A scalable methodology for evaluating and designing coordinated air-traffic flow management strategies under uncertainty," *IEEE Trans. Intell. Transp. Syst.*, vol. 9, no. 4, pp. 644–656, Dec. 2008.
- [9] H. Erzberger and W. Nedell, "Design of automated system for management of arrival traffic," Nat. Aeronautics Space Admin., Moffett Field, CA, Tech. Memo. 102201, Jun. 1989.
- [10] R. W. Schwab, A. Haraldsdottir, and A. W. Warren, "A requirements-based CNS/ATM architecture," presented at the World Aviation Conf., Anaheim, CA, Sep. 28–29, 1998, AIAA Paper 985552.
- [11] J. K. Kuchar and L. C. Yang, "A review of conflict detection and resolution modeling methods," *IEEE Trans. Intell. Transp. Syst.*, vol. 1, no. 4, pp. 179–189, Dec. 2000.
- [12] A. M. Bayen, P. Grieder, H. Sipma, G. Meyer, and C. J. Tomlin, "Delay predictive models of the national airspace system using hybrid control theory," in *Proc. AIAA Guid., Navigat., Control Conf.*, 2002, pp. 767–772.
- [13] B. Shridar and G. B. Chatterji, "Computationally efficient conflict detection methods for air traffic management," in *Proc. ACC*, Albuquerque, NM, 1997, pp. 1126–1130.
- [14] S. Devasia and G. Meyer, "Automated conflict resolution procedures for air traffic management," in *Proc. 36th Conf. Decision Control*, Phoenix, AZ, Dec. 1999, pp. 2456–2462.
- [15] N. Durand, J. Alliot, and O. Chansou, "An optimizing conflict solver for ATC," *Air Traffic Control Quart.*, vol. 3, no. 3, pp. 139–161, 1995.
- [16] Y.-J. Chiang, J. T. Klosowski, C. Lee, and J. S. B. Mitchell, "Geometric algorithms for conflict detection/resolution in air traffic management," in *Proc. 36th IEEE CDC*, San Diego, CA, 1997, pp. 1835–1840.
- [17] P. K. Menon, G. D. Sweriduk, and B. Sridhar, "Optimal strategies for free-flight air traffic conflict resolution," *J. Guid. Control Dyn.*, vol. 22, no. 2, pp. 203–211, 1999.
- [18] K. J. Viets and C. G. Ball, "Validating a future operational concept for en route air traffic control," *IEEE Trans. Intell. Transp. Syst.*, vol. 2, no. 2, pp. 63–71, Jun. 2001.
- [19] D. Dugail, E. Feron, and K. D. Bilimoria, "Conflict-free conformance to en route flow rate constraints," in *Proc. AIAA Guid., Navigat., Control Conf.*, 2002, pp. 20–27.
- [20] J. P. Wangermann and R. F. Stengel, "Optimization and coordination of multiagent systems using principled negotiation," *J. Guid. Control Dyn.*, vol. 22, no. 1, pp. 43–50, Jan./Feb. 1999.
- [21] A. L. Visintini, W. Glover, J. Lygeros, and J. Maciejowski, "Monte Carlo optimization for conflict resolution in air traffic control," *IEEE Trans. Intell. Transp. Syst.*, vol. 7, no. 4, pp. 470–482, Dec. 2006.
- [22] L. Pallottino, E. M. Feron, and A. Bicchi, "Conflict resolution problems for air traffic management systems solved with mixed integer programming," *IEEE Trans. Intell. Transp. Syst.*, vol. 3, no. 1, pp. 3–11, Mar. 2002.
- [23] Z.-H. Mao, D. Dugail, E. Feron, and K. Bilimoria, "Stability of intersecting aircraft flows using heading-change maneuvers for conflict avoidance," *IEEE Trans. Intell. Transp. Syst.*, vol. 6, no. 4, pp. 357–369, Dec. 2005.
- [24] C. Tomlin, I. Mitchell, and R. Ghosh, "Safety verification of conflict resolution maneuvers," *IEEE Trans. Intell. Transp. Syst.*, vol. 2, no. 2, pp. 110–120, Jun. 2001.
- [25] Z.-H. Mao, D. Dugail, and E. Feron, "Space partition for conflict resolution of intersecting flows of mobile agents," *IEEE Trans. Intell. Transp. Syst.*, vol. 8, no. 3, pp. 512–527, Sep. 2007.
- [26] E. Frazzoli, Z.-H. Mao, J.-H. Oh, and E. Feron, "Resolution of conflicts involving many aircraft via semidefinite programming," *J. Guid. Control Dyn.*, vol. 24, no. 1, pp. 79–86, Jan./Feb. 2001.
- [27] A. M. Bayen, R. L. Raffard, and C. J. Tomlin, "Adjoint-based control of a new Eulerian network model of air traffic flow," *IEEE Trans. Control Syst. Technol.*, vol. 14, no. 5, pp. 804–818, Sep. 2006.
- [28] J. Prete, J. Krozel, J. Mitchell, J. Kim, and J. Zou, "Flexible, performance-based route planning for super-dense operations," in *Proc. AIAA Guid., Navigat., Control Conf.*, Honolulu, HI, Aug. 18–21, 2008, pp. 1–14.
- [29] J. Krozel, S. Penny, J. Prete, and J. Mitchell, "Automated route generation for avoiding deterministic weather in transition airspace," *J. Guid. Control Dyn.*, vol. 30, no. 1, pp. 144–153, Jan./Feb. 2007.
- [30] D. Iamratanakul, G. Meyer, G. B. Chatterji, and S. Devasia, "Quantification of airspace sector capacity using decentralized conflict resolution procedures," in *Proc. Conf. Decision Control*, Paradise Island, Bahamas, Dec. 14–17, 2004, pp. 2003–2009.

- [31] S. Devasia, M. Heymann, and G. Meyer, "Automated procedures for air traffic management: A token-based approach," in *Proc. Amer. Control Conf.*, Anchorage, AK, May 8–10, 2002, pp. 736–741.
- [32] Y. Eun, I. Hwang, and H. Bang, "Optimal arrival flight sequencing and scheduling using discrete airborne delays," *IEEE Trans. Intell. Transp. Syst.*, vol. 11, no. 2, pp. 359–373, Jun. 2010.
- [33] H. Erzberger, "Design principles and algorithms for automated air traffic management," AGARD Lecture Series No. 200, Knowledge-Based Functions in Aerospace Systems, San Francisco, CA, Nov. 1995.
- [34] J. Hu, M. Prandini, and S. Sastry, "Optimal coordinated maneuvers for three-dimensional aircraft conflict resolution," *J. Guid. Control Dyn.*, vol. 25, no. 5, pp. 888–900, Sep./Oct. 2002.
- [35] W. P. Niedringhaus, "Stream option manager: Automated integration of aircraft separation, merging, stream management, and other air traffic control functions," *IEEE Trans. Syst., Man, Cybern.*, vol. 25, no. 9, pp. 1269–1280, Sep. 1995.
- [36] F. C. Holland, R. A. Rucker, and B. M. Horowitz, "Structure of the airspace," *IEEE Trans. Commun.*, vol. COM-21, no. 5, pp. 382–398, May 1973.
- [37] J. E. Robinson, III, and D. R. Isaacson, "A concurrent sequencing and deconflicting algorithm for terminal area air traffic control," in *Proc. AIAA Guid., Navigat., Control Conf.*, Denver, CO, Aug. 14–17, 2000, pp. 1–11.
- [38] K. Treleven and Z.-H. Mao, "Conflict resolution and traffic complexity of multiple intersecting flows of aircraft," *IEEE Trans. Intell. Transp. Syst.*, vol. 9, no. 4, pp. 633–643, Dec. 2008.
- [39] J. Yoo and S. Devasia, "Flow-capacity-maintaining, decentralized, conflict resolution with aircraft turn dynamics," in *Proc. Amer. Control Conf.*, San Francisco, CA, Jun. 29–Jul. 1, 2010.



Santosh Devasia received the B.Tech. (Hons.) degree from the Indian Institute of Technology, Kharagpur, India, in 1988 and the M.S. and Ph.D. degrees in mechanical engineering from the University of California, Santa Barbara, in 1990 and 1993, respectively.

From 1994 to 2000, he was with the Mechanical Engineering Department, University of Utah, Salt Lake City. Since 2000, he has been a Professor with the Mechanical Engineering Department, University of Washington, Seattle. His current research interests

include inversion-based control theory and applications such as high-precision positioning systems used in nanotechnology, biomedical applications such as the imaging of human cells to investigate cell locomotion, and control of distributed systems such as air traffic management.



Dhanakorn Iamratanakul received the B.Eng. (First Hon.) degree in aerospace engineering from Kasetsart University, Bangkok, Thailand, in 1999, the M.S. degree in aerospace engineering from the University of Southern California, Los Angeles, in 2000, and the Ph.D. degree in aeronautics and astronautics from the University of Washington, Seattle, in 2007, respectively.

In 2007, he joined Western Digital Corp., where he is currently a Senior Firmware Engineer. He is also with the University of Washington, Seattle. His current research interests include control design for disk-drive servo systems, inversion-based control theory, output-transition control, and the control of complex distributed systems such as air traffic management.



Gano Chatterji received the B.Tech. degree in mechanical engineering from the Indian Institute of Technology, Kanpur, India, the M.S. degree in engineering science from the University of Mississippi, Oxford, and the Ph.D. degree in mechanical engineering from Santa Clara University, Santa Clara, CA.

He is now with the University of California, Santa Cruz, as a Scientist with the Ames Research Center, National Aeronautics and Space Administration (NASA), Moffett Field, CA.

Dr. Chatterji is an Associate Fellow of the American Institute of Aeronautics and Astronautics (AIAA). He has received several awards from NASA and Raytheon for his contribution to the Future Air Traffic Management Concepts Evaluation Tool. Dr. Chatterji has received the IEEE M. Barry Carlton Award and the AIAA Aerospace Software Engineering Award.



George Meyer (LF'09) received the B.S., M.S., and Ph.D. degrees in electrical engineering from the University of California, Berkeley, in 1957, 1960, and 1965, respectively.

He was with the Ames Research Center, National Aeronautics and Space Administration (NASA), Moffett Field, CA, from 1963 through his retirement in 2005. He finds retirement to be surprisingly delightful. His research focused on spacecraft attitude control, aircraft flight control, and air traffic control. This research was typically done in collaboration

with universities through research grants.

Dr. Meyer received awards from NASA and IEEE for his contributions to nonlinear control theory.